point between the highly resistive and the conducting state. In some cases, relaxation oscillations governed by the load resistor and the unit's capacitance ($C \approx 3$ pF) have been observed.

[8]By changing the film thickness, values of V_t between 2.5 and 300 V have been obtained.

[9]Nichrome electrodes yield a particularly low value, $V_h = 0.5$ V. A more detailed study is in progress.

[10]H. Fritzsche, private communication.

[11]K. W. Böer, E. Jahne, and E. Neubauer, Phys. Status Solidi 1, 231 (1961).

[12]B. K. Ridley, Proc. Phys. Soc. (London) 81, 996 (1963).

[13]M. H. Cohen, to be published.

[14]This unit is not the one used for Figs. 1 and 2.

[15]M. H. Cohen, R. G. Neale, and S. R. Ovshinsky, to be published.

[16]G. A. Dussel and R. H. Bubé, J. Appl. Phys. 37, 2797 (1966).

[17]S. R. Ovshinsky, to be published.

SECOND-ORDER STARK EFFECT OF A RESONANT MODE IN NaI:Cl^- †

B. P. Clayman and A. J. Sievers
Laboratory of Atomic and Solid State Physics, Cornell University, Ithaca, New York 14850
(Received 16 September 1968)

The anharmonicity associated with a lattice resonant mode has been identified by means of a second-order Stark-effect measurement.

Large frequency shifts of a lattice resonant mode[1] in NaI:Cl^- caused by an external-electric-field perturbation have been observed.[2] These frequency shifts determine the symmetry of the defect site and give a direct measure of the anharmonicity of the interionic potential for the impurity ion. Although large electric-field–induced shifts have been predicted[3] and observed[4] previously for a defect-induced tunneling mode, such shifts have not yet been reported for local,[5] gap, or resonant modes.[6]

The far-infrared absorption measurements were made using a Strong-type lamellar interferometer and a He^3-cooled bolometer detector[1]; instrumental resolution was 0.2 cm^{-1}. To maintain a uniform electric field across the sample, a special sample configuration has been devised. The doped sample is framed by four pieces of pure crystal so that the fringing fields occur mostly in the pure crystal, and the field on the sample is as uniform as possible. Sample thickness is about 1.4 mm. Two such samples are mounted with the high-voltage electrode between them. Up to 12 kV could be applied without electrical breakdown. Incident radiation is polarized by a 500-lines/in. Ni grid deposited on Mylar film[7] placed in the light path just before the sample.

The transmission spectrum of the sample was measured for several different values of electric field E_{dc} applied in the [100] and [110] crystal directions, for incident radiation polarized both perpendicular and parallel to the dc electric field. The frequency of the E-shifted line was determined by dividing the transmission spectrum by the zero-field unshifted spectrum and forming the absorption constant $\alpha(E, \omega)$ from

$$I(E, \omega) = I(0, \omega) \exp[-\alpha(E, \omega)t],$$

where $I(E, \omega)$ and $I(0, \omega)$ are the transmitted intensities for E- and zero-field, respectively, at frequency ω, and t is the sample thickness. The absorption constant of the unperturbed line was then added to $\alpha(E, \omega)$. This indirect process is necessitated by the difficulty of making a pure sample which has a geometry, hence an optical interference pattern, identical to that of the doped sample.

Typical results of this data reduction process are shown in Fig. 1 for the case of $E_{ir} \| E_{dc} \| [100]$, where ir denotes infrared. Applied volt-

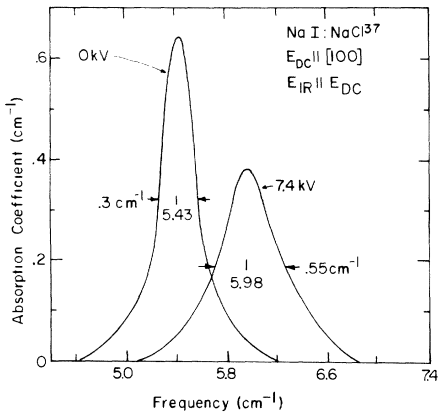

FIG. 1. Typical electric-field–induced frequency shift. Instrumental resolution is 0.2 cm^{-1}.

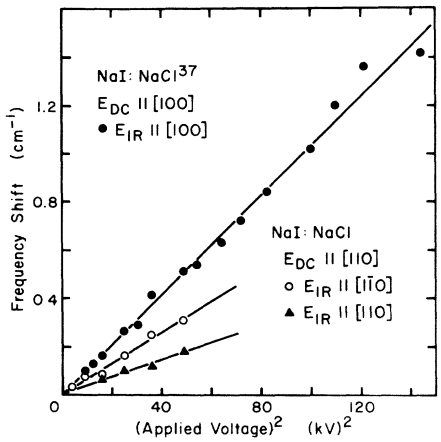

FIG. 2. Summary of second-order Stark-effect results. The frequency shift is plotted versus the square of the applied voltage.

age is 7.4 kV. The absorption line shifts upward in frequency and broadens considerably upon application of the field.

The measured shifts are summarized in Fig. 2 for both $E_{dc} \| [100]$ and $E_{dc} \| [110]$. The shift for $E_{ir} \| [001]$ in both cases is very small ($|\Delta\omega| \leq 0.01$ cm^{-1} for 64 kV/cm applied external [100] field) and is negative. The frequency of the unperturbed line for $E_{dc} \| [110]$ in Fig. 2 is 5.537 cm^{-1}; natural-abundance chlorine dopant was used for this sample. From $E_{dc} \| [100]$, the frequency shift is found to be proportional to V^n, where V is applied voltage and $n = 2.0 \pm 0.1$.

The width of the line at half-maximum absorption increases from about 0.3 cm^{-1} at zero field to more than 1.0 cm^{-1} at 12-kV applied voltage for the measurements shown in Fig. 2. However, no broadening is observed for $E_{ir} \| [001]$. We attribute the broadening of the line to nonuniformity of the applied electric field, caused by fringing fields and surface imperfections.

The most significant result of these experiments is the large (up to 25%) field-induced change in the resonant-mode frequency. The polarization dependence of these quadratic shifts identifies the defect-site symmetry. Because the second-order Stark-effect and the uniaxial-stress perturbation operators have the same symmetry properties, the same polarization selection rules apply to both.[8] By inspection,[9] only a cubic defect site is consistent with the experimental results: that is, results in two lines of equal intensity for the two E_{ir} polarizations when $E_{dc} \| [100]$ and three lines of equal intensity for the three E_{ir} polarizations when $E_{dc} \| [110]$. The only cubic site in the NaCl-type lattice which has inversion symmetry (deduced from the quadratic shift) is O_h.

We can obtain a measure of the anharmonicity of the potential experienced by the Cl^- ion by treating the resonant mode as a perturbed harmonic oscillator. Because of the extremely low frequency of the resonant mode, the eigenvector will consist of long-wavelength oscillations of the neighboring ions π out of phase with the Cl^- ion. Therefore, in this normal mode, the motion of the Cl^- ion is expressed in terms of its relative coordinates (x, y, z) with respect to the center of mass of the surrounding lattice. The potential energy of the Cl^- ion in a potential of O_h symmetry can be expanded[10] as

$$V(x,y,z) = \tfrac{1}{2}m\Omega^2(x^2+y^2+z^2) + \beta(x^4+y^4+z^4) + \gamma(x^2y^2+y^2z^2+z^2x^2) + \cdots, \quad (1)$$

where m is the reduced mass. From the previous isotope-shift measurement,[1] the reduced mass must be set equal to the Cl^- ion mass. This result is consistent with the idea of the Cl^- ion bonds flexing against the rest of the lattice in the resonant mode; for then $m(\text{lattice}) \to \infty$ and $1/m = [1/m(Cl^-) + 1/m(\text{lattice})] \to 1/m(Cl^-)$. This model predicts an A_{1g} ground state and a triply degenerate T_{1u} first excited state as expected. The unperturbed $A_{1g} \to T_{1u}$ transition energy (which we identify with the resonant-mode transition at 5.4 cm^{-1}) for this anharmonic oscillator is

$$\epsilon = \hbar\Omega + (3\beta+\gamma)(\hbar/m\Omega)^2. \quad (2)$$

By means of second-order perturbation theory, we can relate the observed shifts $\Delta\epsilon$ with applied field to the coefficients β, γ, and Ω in Eq. (1). We retain only terms of lowest order in E^2, β, and γ, and find the predicted shifts in transition energies. These are listed in Table I in units of $\hbar(eE)^2/8m^3\Omega^5$. Here eE is the product of the effective impurity charge and the local electric field.

Also listed in Table I are the slopes of the linear fits in Fig. 2. These slopes should be proportional to the coefficients listed in the third column of the table. For the [110] sample, we see that

$$\frac{\Delta\epsilon[110]-\Delta\epsilon[001]}{\Delta\epsilon[1\bar{1}0]} = \frac{18\beta+8\gamma-8\gamma}{30\beta} = \frac{18\beta}{30\beta} = 0.60 \text{ (calc)}.$$

Table I. Tabulation of second-order Stark-effect results.

Polarization E_{dc}	Polarization E_{ir}	Calculated shifts $\Delta\epsilon$ $[\hbar(eE)^2/8m^3\Omega^5]$	Experimental slopes $\times 10^2$ (cm^{-1}/kV^2)
100	100	48β	1.04 ± 0.02
100	001	8γ	$\sim -0.02 \pm 0.01$
110	110	$18\beta + 8\gamma$	0.36 ± 0.02
110	110	30β	0.63 ± 0.02
110	001	8γ	$\sim -0.01 \pm 0.005$

The experimental value for this quantity is 0.59 ± 0.05. This close agreement indicates that the error in neglecting higher-order terms in the perturbation calculation and in the expansion of the potential energy is negligible.

To evaluate β, γ, and Ω numerically, knowledge of the local field at the resonant-mode site is needed. Recently, Mahan[11] has shown that the local field at a defect site should be written as

$$E = \tfrac{1}{3}(\epsilon_S + 2)[1 - g\alpha(\alpha - \alpha')]E_0, \quad (3)$$

where E is the local field, E_0 the applied field, ϵ_S the dielectric constant, α and α' the total (electronic and ionic) polarizabilities of the host and impurity ions, respectively, and g is a complicated wave-vector sum which has not yet been evaluated. We note that for $\alpha' = \alpha$ Eq. (3) reduces to the well known Lorentz correction.

The following approach is used to estimate the local field from Eq. (3):

(1) The factor $g\alpha^2$ is evaluated by using the Onsager local field $E = [3\epsilon_S/(2\epsilon_S + 1)]E_0$ for a nonpolarizable impurity, $\alpha' = 0$.

(2) The ionic polarizability of the resonant mode is estimated from

$$\alpha'(\text{ionic}) = (\mu\omega_\gamma^2/m\Omega_0^2) f \alpha_{\text{NaI}}(\text{ionic}),$$

where ω_γ is the TO mode at $k = 0$, μ is the reduced mass for NaI, m is the Cl^- mass, Ω_0 is the resonant-mode frequency, and f is the oscillator strength[12] of the resonant mode.

(3) The two components to the electronic polarizability α'(electronic) are identified as the contribution from the Cl^- ion and the contribution from the large number of neighbors of average polarizability $\frac{1}{2}(\alpha_{\text{Na}} + \alpha_{\text{I}})$.

The total polarizability which we use in Eq. (3) is then

$$\alpha' = \left(\frac{\mu\omega_\gamma^2}{m\Omega_0^2} f \alpha_{\text{NaI}}\right)_{\text{ionic}} + (\alpha_{Cl^-} + \tfrac{1}{2}\alpha_{\text{NaI}})_{\text{electronic}},$$

and the local field is

$$E \approx 2.4 E_0.$$

We assume the unperturbed electronic charge for the Cl^- impurity and use the approximate local-field correction found above. By substituting the appropriate measured values of ϵ and $\Delta\epsilon(E)$ into Eq. (2) and into the expressions for $\Delta\epsilon$, we obtain the following values for β, γ, and Ω:

$$\beta = 8.54 \times 10^{16} \text{ erg/cm}^4,$$

$$\gamma = -0.16 \times 10^{16} \text{ erg/cm}^4,$$

$$\Omega = 9.61 \times 10^{11} \text{ sec}^{-1}.$$

Substituting these numerical results into Eq. (2), we see that the anharmonic contribution to the transition energy is only about 7 %.

Now we can also predict the Cl^- isotope shift for the system from Eq. (2):

$$\epsilon(35)/\epsilon(37) = 1.030.$$

This value is consistent with the experimentally determined value of

$$\epsilon(35)/\epsilon(37) = 1.029 \pm 0.008$$

estimated in Ref. 1.

No doubt a more complete analysis of the local-field correction is required for a quantitative determination of the anharmonicity parameters. However, despite this difficulty, our investigation has demonstrated that the second-order Stark effect is an important probe of the lattice potential associated with low-frequency defect modes.

---

†Work supported primarily by the U. S. Atomic Energy Commission under Contract No. AT(30-1)-2391, Technical Report No. NYO-2391-87. Additional support was received from the Advanced Research Projects Agency through the Materials Science Center at Cornell University, Report No. 1031.

[1]B. P. Clayman, I. G. Nolt, and A. J. Sievers, to be published.

[2]Some preliminary results have been reported. B. P. Clayman and A. J. Sievers, Bull. Am. Phys. Soc. 13, 659 (1968).
[3]M. Gomez, S. P. Bowen, and J. A. Krumhansl, Phys. Rev. 153, 1009 (1967).
[4]R. A. Herendeen, Bull. Am. Phys. Soc. 13, 660 (1968); G. Höcherl and H. C. Wolf, Phys. Letters 27A, 133 (1968).
[5]W. Hayes and H. F. Macdonald, Proc. Roy. Soc. (London), Ser. A 297, 503 (1967).
[6]R. D. Kirby and A. J. Sievers, to be published.
[7]Buckbee-Meers Company, Minneapolis, Minnesota.
[8]W. Gebhardt, Phys. Rev. 159, 726 (1967).
[9]D. B. Fitchen, in Physics of Color Centers, edited by W. B. Fowler (Academic Press, Inc., New York, 1968), Chap. 5.
[10]Elliott et al. have used a somewhat similar model to describe the U center in CaF_2; see R. J. Elliott, W. Hayes, G. D. Jones, H. F. Macdonald, and C. T. Sennett, Proc. Roy. Soc. (London), Ser. A 289, 1 (1965).
[11]G. D. Mahan, Phys. Rev. 153, 983 (1967).
[12]I. G. Nolt, R. A. Westwig, R. W. Alexander, Jr., and A. J. Sievers, Phys. Rev. 157, 730 (1967).

ISOBARIC ANALOG RESONANCES IN STRIPPING AND PICKUP REACTIONS*

Nelson Stein, J. P. Coffin,† C. A. Whitten, Jr., and D. A. Bromley
Wright Nuclear Structure Laboratory, Physics Department, Yale University, New Haven, Connecticut
(Received 14 August 1968)

Resonance structure is observed in many (d,p) and (p,d) excitation functions in the lead region. The results are compared with previously reported (t,p), (p,t), and (d,p) data, and systematic resonance behavior is found common to all stripping and pickup reactions involving incident or final protons. Resonances occur whenever the proton-channel energies lie between 16 and 18 MeV. This is the energy region where single-particle isobaric analog states occur in the reaction $Pb^{208}(p,p)$.

Isobaric analog states in heavy nuclei have been widely studied by proton elastic and inelastic scattering.[1] Recently, resonances observed in certain (d,p), (p,d), and (t,p) excitation functions from targets in the lead region also have been identified with isobaric analog states.[2-5] However, unlike proton scattering for which many aspects of the analog-resonance phenomenon are reasonably well established and understood, in neutron-transfer reactions neither a clear theoretical understanding nor a firm experimental basis for the occurrence of such resonances has yet been offered. In this Letter results are presented from a study of the reactions $Pb^{208}(p,d)$, $Pb^{207}(d,p)$, and $Pb^{206}(d,p)$ as a function of energy. In the excitation function for almost every transition studied thus far, we find resonance structure that is clearly associated with isobaric analog states. From these results, certain systematic features of analog resonances in transfer reactions in the lead region are readily apparent, and all of the presently available data, including the earlier work mentioned above, can be correlated. The essential feature is the location of the resonance structure in approximately the same region of proton-channel energies for all transitions studied, independent of target nucleus, Q value, final state, or the particular reaction used. These results are important for understanding (1) the isobaric-analog-resonance mechanism, (2) the nature and identity of the isobaric analog states responsible for the resonances, and (3) the relationship between the resonances in the (p,d), (d,p), and (t,p) transfer reactions and the more familiar (p,p) and (p,p') resonances.

The experiments were performed using proton and deuteron beams from the High Voltage Engineering Corporation Model MP tandem accelerator at Yale. The measurements were made with standard solid-state detector systems. Excitation functions measured at 165° for the reaction $Pb^{208}(p,d)$ leading to the first five neutron-hole states of Pb^{207} are presented in Fig. 1. Strong resonance structure can be seen for incident proton energies between 16 and 18 MeV. These are the same incident energies where strong isobaric analog resonances have been observed[6,7] in proton scattering on Pb^{208} corresponding to the $3d_{5/2}$, $4s_{1/2}$, $2g_{7/2}$, and $3d_{3/2}$ single-particle states in Pb^{209}. More detailed measurements[4] near $E_p = 15$ MeV confirm the relatively small resonance effects (~10%), attributed to the $2g_{9/2}$ single-particle analog state, in the first three (p,d) excitation functions.

Excitation functions for the reaction $Pb^{207}(d,p)$